Electronic Journal of Structural Engineering

Original Article

Cite this: DOI:10.56748/ejse.26889

Received Date:25 September 2025
Accepted Date: 22 February 2026

1443-9255
https://ejsei.com/ejse

Reactivity of fine particles in incineration bottom ash for supplementary cementitious materials

Yongzhen Cheng [a*], Weiye Mu [a]

[a] Faculty of Architecture and Civil Engineering, Huaiyin Institute of Technology, No. 89 Beijing North Road, Huai'an 223001, China
*Corresponding author: chengyongzhen198@163.com

Abstract

The high-value exploitation of municipal solid waste incineration bottom ash can be achieved by reducing its particle size to serve as a substitute for cement. This study uncovers the reactivity of fine bottom ash recycled micro-powder (FBA-RMP). In addition, the application of FBA-RMP as a cement substitute in mortar is studied. The results suggest that a certain quantity of active constituents exist in FBA-RMP, wherein SiO_2, CaO, Al_2O_3 and Fe_2O_3 together make up around 85.3 wt.%. Although C-S-H gel and AFt are found in the paste with 30% FBA-RMP replacing cement, there are significant pores, among which the content of large pores is about 19.27%. As a result, the 28-day compressive strength of the mortar is 55.0% lower than that of the reference mortar. However, decreasing the proportion of FBA-RMP or extending the curing days can remarkably enhance mortar strength.

Keywords

Incineration bottom ash, Fine particles, Physical and chemical properties, Hydration products, Pore structure

1. Introduction

1.1 Research background

Municipal solid waste generation in China keeps rising. In 2023 alone, 196 large and medium-sized cities produced 254 million tons of domestic waste, with 209 million tons treated through incineration (NBS, 2023). Similar municipal solid waste management challenges exist globally. For example, unscientific disposal in Jalandhar, India, has caused severe environmental and social problems (Singh and Kumar, 2023). Traditional landfill methods easily create potential environmental pollution risks, making incineration a popular alternative for waste treatment with heat energy recovery. By 2019, China had 405 operational waste-to-energy plants. Incineration reduces municipal solid waste mass by about 70% and volume by up to 90%, achieving initial waste reduction and harmless treatment. The generated heat can be used for power generation to realize effective energy recovery (Sisani et al., 2022; Abd Kadir et al., 2013; Bosmans et al., 2013).

Municipal solid waste incineration bottom ash is discharged from the end of the furnace. To protect the environment, ferrous and non-ferrous metals are first removed through electromagnetic eddy current treatment. Bottom ash particles mainly consist of glass, ceramics and sand with diverse components. With the rapid growth of waste incineration, large-scale accumulation of bottom ash has become an urgent issue. Resource utilization is an effective way to reduce its landfill volume. Its gradation is similar to natural sand, so it is suitable as fine aggregate in concrete (Rehman et al., 2020; Yan et al., 2020). Its porous and lightweight properties make it fit for lightweight concrete production. More importantly, its fine ground powder can replace cement, reduce cement consumption and contribute to environmental protection and infrastructure sustainability (Fialova et al., 2019; Kleib et al., 2021).

Large-scale accumulation of bottom ash not only occupies considerable land resources but also brings potential environmental risks such as heavy metal leaching. Exploring efficient resource utilization pathways has thus become a research focus in recent years (Singh and Kumar, 2022). Previous studies show that proper stabilization treatment is necessary before bottom ash application to ensure environmental safety and performance stability (Singh and Kumar, 2022).

1.2 Literature review

Over the past five years, extensive studies have been conducted on the resource utilization of municipal solid waste incineration bottom ash. These studies cover multiple fields including aggregate application, property optimization, environmental safety and basic characteristic research, providing rich theoretical and experimental support for large-scale recycling (Jin et al., 2024; Kumar and Singh, 2021). Among these fields, application as an aggregate in construction and geotechnical engineering has attracted significant research attention. Bottom ash can completely replace natural silica sand for preparing engineered cementitious composites (Liu et al., 2024a). Although such composites show increased porosity, appropriate fiber dosage significantly enhances their flexural strength. Further verification confirms that using 100% bottom ash as fine aggregate in ECCs with optimized polymer fiber content improves deformation capacity and toughness, while heavy metal solidification efficiency reaches 97% (Liu et al., 2024b).

For artificial lightweight aggregate preparation, cold-bonded granulation technology enables the production of eco-friendly aggregates with over 50% bottom ash, less than 50% fly ash or ground granulated blast furnace slag, and 10% ordinary Portland cement. These aggregates have compressive strength exceeding 2.5 MPa and bulk density around 1000 kg/m^3, offering a new pathway for large-scale bottom ash recycling (Jin et al., 2024). In sprayed mortar production, bottom ash can serve as fine aggregate. Orthogonal tests help optimize the mix ratio, and the prepared lightweight sprayed mortar achieves a 1-day unconfined compressive strength of 18.5 to 31.3 MPa (2.6 to 4.5 times the standard). Supplementary cementitious materials can further improve this strength (Liu et al., 2024a; Liu et al., 2025).

In geotechnical and stabilization applications, cement stabilization of bottom ash forms C-S-H, C-A-H gels and calcium hydrates. This process significantly improves mechanical properties and traps heavy metals. Adding 7% binder and 1% fiber optimizes bottom ash composite performance for road construction, with leaching performance meeting relevant standards (Kumar and Singh, 2023; Kumar and Singh, 2024).

Particle size is a key factor affecting bottom ash performance in cement-based materials. Extensive research has also focused on the physical and chemical properties and stabilization of bottom ash. Incorporating bottom ash adjusts pore structure by increasing micropores, reducing mesopores and enlarging macropores. Smaller particles rich in aluminum and calcium carbonate promote early hydration and carbonation (Cheng et al., 2024a). Regarding physical and chemical properties and stabilization, multiple tests confirm the heterogeneity of bottom ash and emphasize the need for stabilization before application. Researchers have also summarized its application potential in construction and soil improvement, noting promising prospects in aggregate substitution and new compound synthesis (Singh and Kumar, 2022; Kumar and Singh, 2021).

Environmental safety is essential for bottom ash recycling and has received widespread attention. Relevant studies have systematically explored tannery effluent treatment, regional waste management, landfill site assessment and leachate-induced groundwater pollution. These studies provide critical references for environmental risk control during bottom ash recycling, ensuring environmentally friendly utilization (Sanjeev and Deswal, 2021; Ranjan et al., 2021; Bhardwaj et al., 2023; Kumar and Singh, 2023; Kumar and Singh, 2024).

Notably, early studies on bottom ash are outdated (Lin and Lin, 2006; Yao et al., 2010). These studies generally report low reactivity of untreated bottom ash, which prevents its use as a cement substitute. While recent activation technologies have improved bottom ash reactivity, relevant research remains incomplete and requires further supplementation

(Singh and Kumar, 2022). This research gap lays the foundation for the focus of the current study.

1.3 Research gaps and significance

Despite significant progress in bottom ash resource utilization, obvious research gaps highlight the need for this study. First, most existing studies focus on course or medium bottom ash particles in aggregates, concrete, ECCs and geotechnical engineering. Systematic research on fine particles (0 to 0.6 mm) as supplementary cementitious materials is lacking (Liu et al., 2025). Second, studies on bottom ash reactivity mainly focus on mixed particle activation. In-depth analysis of the intrinsic reactivity of fine particles and their hydration mechanism and structural evolution as cement substitutes remains insufficient (Kleib et al., 2021; Singh and Kumar, 2022). Third, no systematic research exists on the relationship between fine particle characteristics, hydration process, pore structure distribution and mortar strength (Cheng et al., 2024a).

This study holds dual significance. In terms of resource utilization, it explores fine bottom ash particles as supplementary cementitious materials, expanding utilization pathways, reducing landfill volume and realizing high-value solid waste recycling (Jin et al., 2024; Kumar and Singh, 2021). Academically, it clarifies the reactivity and hydration mechanism of fine bottom ash particles, fills research gaps and provides experimental and theoretical support for their rational application (Liu et al., 2025).

1.4 Research objectives

To address the above research gaps, this study focuses on the reactivity of fine municipal solid waste incineration bottom ash particles (0 to 0.6 mm) with the following objectives. First, it systematically investigates the physical and chemical characteristics of fine bottom ash recycled powder through X-ray fluorescence, X-ray diffraction, scanning electron microscopy and laser particle size analysis. Second, it analyzes the hydration properties and structural characteristics of composite binders composed of cement and fine bottom ash recycled powder using X-ray diffraction, scanning electron microscopy, mercury intrusion porosimeter, Fourier transform infrared spectroscopy and thermogravimetry. Finally, it tests the strength of mortar containing fine bottom ash recycled powder as a substitute to evaluate its application feasibility as a supplementary cementitious material.

2. Materials and Methods

2.1 Raw materials and treatment

The bottom ash generated from incinerating municipal solid waste was procured from a power station in Suqian, China. Each year, this facility processes as much as 300,000 tons of municipal solid waste. The collected municipal solid waste is unsorted and is directly fed into the grate furnace with temperature controlled at 850–950°C after percolation. The residue collected from the furnace tail is separated from non-ferrous and ferrous metals through water shaking and electromagnetic vortex current. Afterwards, it is stored in the slag pool, which is referred to as bottom ash.

The sampled bottom ash was pretreated by water immersion to remove impurities (plant roots, grass pieces, plastic products); during this process, some fine dust with higher contents of Cl, SO_3 and metal ions was also discharged along with these impurities, followed by air-drying and sieving to obtain particles of different sizes. The particle distribution of municipal solid waste incineration bottom ash is shown in Fig. 1. The bottom ash particles are primarily within the range of 0 to 4.75 mm, with very few particles of 9.5 mm in size. Particles having a size of 1.18-2.36 mm account for a relatively high proportion of the bottom ash. The particles sized 0-0.6 mm make up approximately 27% by weight, and these fine particles were selected for analysis in this study to uncover their particle composition, chemical constituents, physicochemical properties and reactivity.

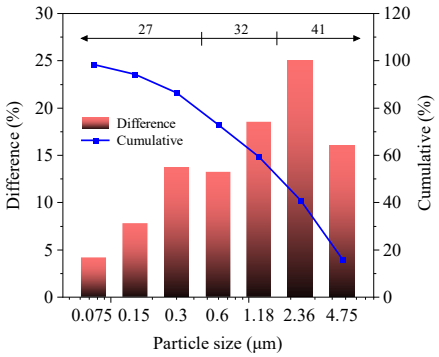

Fig. 1 Particle distribution of municipal solid waste incineration bottom ash

A planetary ball mill with a velocity fixed at 350 r/min was employed to grind the fine bottom ash particles for 45 minutes, obtaining a dark-gray powder with a particle size not exceeding 75 μm, which was labeled as FBA-RMP.

Portland cement Type II (P·II 52.5) was used, which contains up to 5% limestone or granulated blast furnace slag as supplementary components. The employment of P·II cement helps to verify the reactivity of FBA-RMP and its influence on cement hydration. The ISO standard sand utilized had a particle size spanning from 0 to 2 mm and fulfilled the criteria specified in the Chinese standard (GB/T 17671, 2021), ensuring the reliability and consistency of the experimental materials.

2.2 Test methods

XRD (Cu target, 40 kV, 36 mA, 4°/min) served to examine the mineral ingredients of FBA-RMP. XRF (MnKa resolution<155ev, CPS>3000) served to determine the chemical components of FBA-RMP. Microtrac S3500 laser particle size meter served to measure the particle distribution of FBA-RMP. NanoSEM NPE218 SEM served to survey the microscopic morphology of FBA-RMP.

The cement paste was prepared according to the specified mix ratio, with detailed sample design and mix ratio shown in Table 1. Specifically, the fresh paste samples were injected into a centrifuge tube and cured at 20°C for 28 days. Then, the solidified paste was cracked and immersed in anhydrous ethanol for 24 hours. This process was repeated several times to terminate cement hydration. Next, the samples were placed in an oven to dry at 40°C. Some samples were ground until free of graininess. Afterwards, XRD, FTIR, and TG were used to identify the minerals in the paste derived from the hydration of cementitious materials. Finally, an Autopore IV9510 mercury porosimeter was used to determine the pore structure of the paste samples.

Table 1. Sample Design and Mix Ratio Details

Samples	Binder	Sand	Water/ Binder Ratio	FBA-RMP: cement	Curing condition	Curing days
Cement paste	1	-	0.5	3:7	20°C, in centrifuge tubes	28
Mortar	1	3	0.5	1:9	Immersed in water at (20±2) °C	3; 28; 90
	1	3	0.5	2:8	Immersed in water at (20±2) °C	3; 28; 90
	1	3	0.5	3:7	Immersed in water at (20±2) °C	3; 28; 90

Note: Binder refers to the composite cementitious material composed of FBA-RMP and cement.

The mortar was fabricated in accordance with the Chinese standard (GB/T 17671, 2021), with its mix ratio detailed in Table 1. For the triple specimens of mortar, the dosage quality was set as follows: 450g of cementitious material, 1350g of sand, and 225g of water. The fresh mortar was placed into a prismatic mold and cured at room temperature for 24 hours prior to demolding. Finally, the mortar samples were cured by immersion in water at (20±2) °C for 3, 28 and 90 days to test their flexural and compressive strengths. Additionally, the strength of mortar without FBA-RMP was tested to analyze the reactivity of fine bottom ash particles. A replacement gradient of 10%, 20% and 30% was designed, and 30% was adopted as the upper limit to investigate the maximum applicable dosage and performance evolution mechanism of FBA-RMP as a supplementary cementitious material.

3. Results and Discussion

3.1 Material properties

Particle composition and morphology

The incineration bottom ash particles with a size of 0–0.6 mm are presented in Fig. 2, exhibiting a dark-gray appearance, porous structure, and low bulk density. For a more detailed characterization of particle constituents, Fig. 3 presents a magnified view of primary components, including sand, glass, ceramic particles, and distinct non-homogeneous phases. These non-homogeneous phases are identified as slag particles associated with molten metal oxide phases, and this classification is supported by the subsequent detection of hematite (Fe_2O_3) and magnetite (Fe_3O_4) in the bottom ash. Quantitatively, slag particles (including these non-homogeneous phases) are the most abundant, accounting for approximately 47.0 wt.% of the bottom ash, followed by glass particles (23.8%) and ceramic particles (15.6%). The reactivity of these particle types follows the order: glass > ceramic > mineral > slag.

Chemical properties and mineral composition

The chemical constitution of FBA-RMP is presented in Table 2. The FBA-RMP can be classified into the category of the SiO_2–CaO–Al_2O_3–Fe_2O_3 chemical system, similar to that of cement. Such four oxides make up approximately 85.3% of FBA-RMP. However, the contents of SiO_2, Al_2O_3, and Fe_2O_3 in FBA-RMP are nearly two to three times greater than those in the cement. In contrast, the content of CaO is only approximately one-third of that in the cement. Strangely, the contents of chlorine (Cl) and sulfur trioxide (SO_3) in FBA-RMP are less than one-third of those in cement. This is associated with the treatment of the bottom ash in this study. Due to inadequate incineration of waste or contamination during transportation or storage, the bottom ash has a substantial quantity of plant roots and plastic products. To remove these contaminants, the bottom ash is immersed in water so that the mixed light substances are suspended and discharged. In this process, a large amount of ultra-fine dust in the bottom ash is discharged with water, while Cl and SO_3 often accumulate in such substances (Saffarzadeh et al., 2011). Therefore, the fine bottom ash used in this research is relatively clean, resulting in less Cl and SO_3 in FBA-RMP.

Fig. 2 Incineration bottom ash particles with a size of 0-0.6 mm

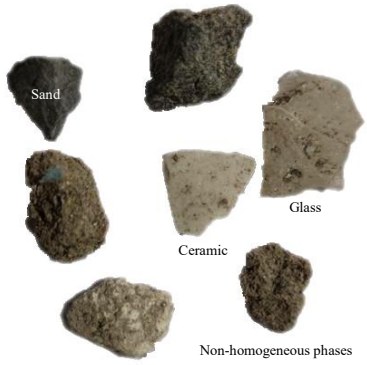

Fig. 3 Particles in incineration bottom ash with a size of 0-0.6 mm

Table 2. Chemical composition of FBA-RMP and P·Ⅱ 52.5 cement (wt.%)

Oxides	MgO	Na_2O	Al_2O_3	SiO_2	P_2O_5	K_2O	CaO
P·Ⅱ 52.5 cement	1.56	0.00	3.80	17.11	0.63	0.16	64.99
FBA-RMP	2.35	2.47	9.33	46.44	3.24	2.53	21.90
Oxides	TiO_2	MnO	Fe_2O_3	CuO	ZnO	Cl	SO_3
P·Ⅱ 52.5 cement	0.27	0.09	3.59	0.02	0.15	2.00	3.96
FBA-RMP	0.86	0.15	7.58	0.17	0.38	0.67	1.13

The mineral composition of FBA-RMP is presented in Fig. 4. Quartz and calcite are identified as the main minerals, and gehlenite, gypsum, magnetite, diopside, and sodium feldspar are also found in FBA-RMP. There is a quite tall peak, which is located at 26.6°, and it can be determined as the principal peak of quartz. Qiao et al (2008) announced an analogous result. This is also highly consistent with the previous chemical analysis which shows that SiO_2 is the most abundant element in FBA-RMP. The calcite in FBA-RMP also has obvious diffraction peaks. As is in line with the previous chemical analysis, it indicates that FBA-RMP contains more CaO.

Particle distribution and morphology of FBA-RMP

Fig. 5 presents the particle distribution of FBA-RMP. The particle size of FBA-RMP ranges from 0.2 to 80 μm. This is because the size of the fine bottom ash particles decreased to obtain micro-powder, which is then passed through a 200-mesh sieve to eliminate impurities and unbroken particles. The median particle size of FBA-RMP is approximately 20 μm, indicating that FBA-RMP has a particle fineness comparable to that of cement. Hence, when FBA-RMP is blended with cement, FBA-RMP will possess a larger contact area with the cement, which proves advantageous for the hydration reaction of the FBA-RMP-cement composite cementitious material. Additionally, the unreacted particles fill the pores of the mortar, helping to improve the compactness of the mixture.

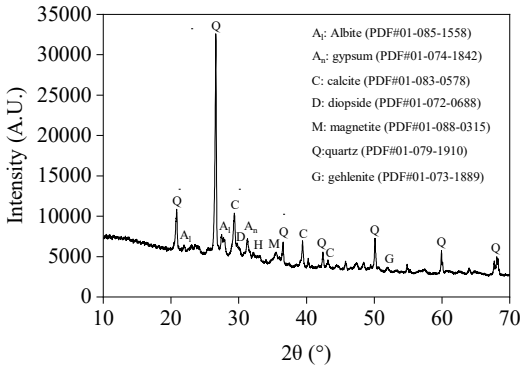

Fig. 4 Mineral composition of FBA-RMP

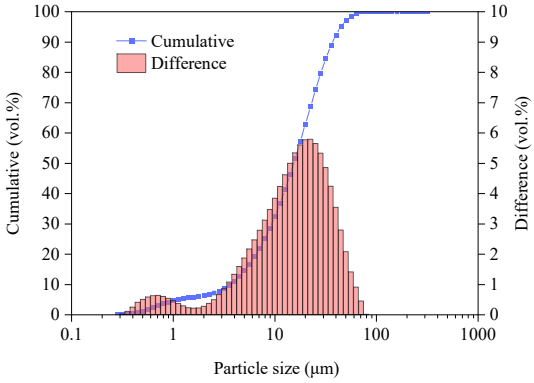

Fig. 5 The particle distribution of FBA-RMP

The microscopic morphology of FBA-RMP is presented in Fig. 6. The particles of FBA-RMP exhibit multiple fracture surfaces, resembling gravel. Moreover, more small particles in the form of flocculation are accumulated around the large particles. Additionally, no spherical particles are found in FBA-RMP, suggesting that it does not possess a water-reducing effect similar to that of fly ash.

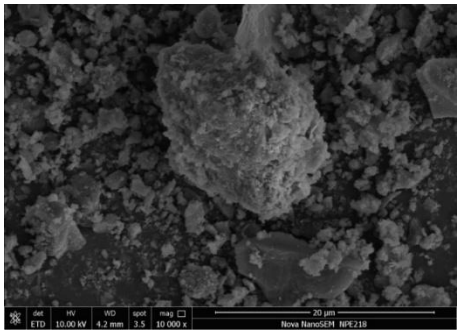

Fig. 6 SEM image of FBA-RMP

3.2 Properties of composite cementitious material

Hydration properties

The contribution of FBA-RMP to cement hydration is analyzed. The XRD pattern of paste with 30% FBA-RMP instead of cement after 28 days of curing is shown in Fig. 7. The main minerals identified in the samples are quartz (silicon dioxide, with the chemical formula SiO_2), calcite (calcium carbonate, with the chemical formula $CaCO_3$), calcium hydroxide (with the chemical formula $Ca(OH)_2$), dicalcium silicate (with the chemical formula $2CaO{\cdot}SiO_2$, abbreviated as C_2S), and tricalcium silicate (with the chemical formula $3CaO{\cdot}SiO_2$, abbreviated as C_3S). Quartz mainly comes from FBA-RMP that does not participate in cement hydration. Dicalcium silicate and tricalcium silicate are hydrolyzed sequentially to produce a large amount of CH. Compared with the XRD patterns of FBA-RMP, the diffraction intensity of calcite in the cement paste is greater and the peak position is more prominent, indicating that the cement paste contains more carbonate than that in FBA-RMP. However, the diffraction peaks of the Calcium Silicate Hydrate (C-S-H) gel, Ettringite (Aft), and Monosulfate (AFm) are not obvious in the XRD patterns of the cement paste.

To determine the presence of such gels in the cement paste, the TG/DTG curves of the cement paste after 28 days of curing were obtained through simultaneous thermal analysis. As shown in Fig. 8, the mass loss near 65 ℃ is attributed to the dehydration of ettringite (AFt). The water loss from the decomposition of C-S-H gel occurs near 95 ℃. The decomposition of calcium aluminosilicate hydrate (C_2ASH_8) occurs near 150 ℃. The mass loss near 470 ℃ corresponds to the water loss from the

decomposition of CH. The decomposition of carbonate occurs near 690–710 °C. The total weight loss of the cement paste is about 23.3%, while the weight loss in the temperature range of 0-150 °C is about 8.6%, which proves the existence of a considerable amount of gel in the cement paste

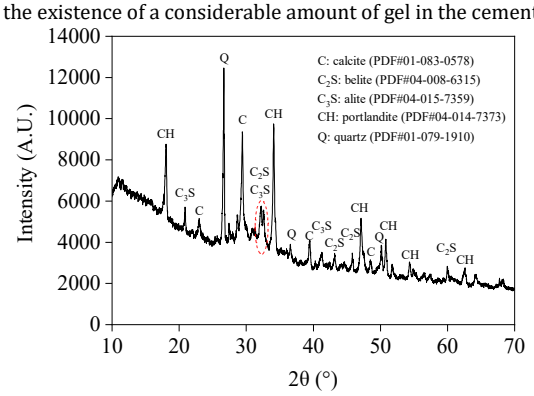

Fig. 7 XRD pattern of the cement paste with 30% FBA-RMP as a replacement of cement after 28 days of curing

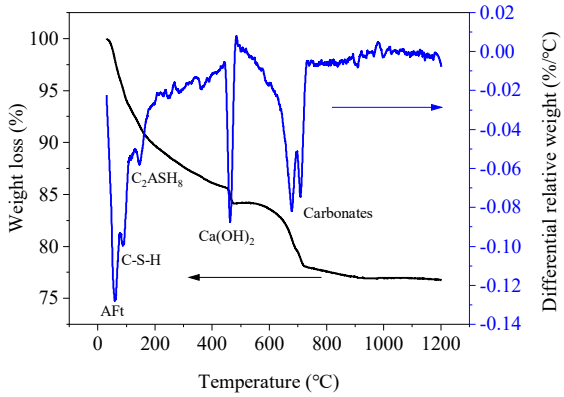

Fig. 8 TG/DTG curves of the cement paste with 30% FBA-RMP replacing cement after 28 days of curing

Fig. 9 presents the FTIR spectra of the cement paste with 30% FBA-RMP instead of cement after 28 days of curing. Based on the literature data (Xu et al., 2018; Li et al., 2019), the main minerals in the cement paste are identified as follows: The stretching vibration of O–H in calcium hydroxide appears at 3645 cm^{-1}. The bending vibration of the H–OH group in crystalline water occurs around 3440 cm^{-1}. Near 1650 cm^{-1}, the C=O groups existing in the cement paste underwent asymmetric vibration. This is attributed to the presence of aromatic substances, carboxylic acids, amino and lipid compounds in FBA-RMP. At 1420 cm^{-1}, The asymmetric stretching vibration corresponds to the presence of carbonates. The stretching vibration of Si–O in the C–S–H phase occurs close to 970 cm^{-1}. The formation of these hydration products indirectly demonstrates the potential pozzolanic activity of FBA-RMP, which is further quantitatively characterized by the activity index in the subsequent mortar property analysis.

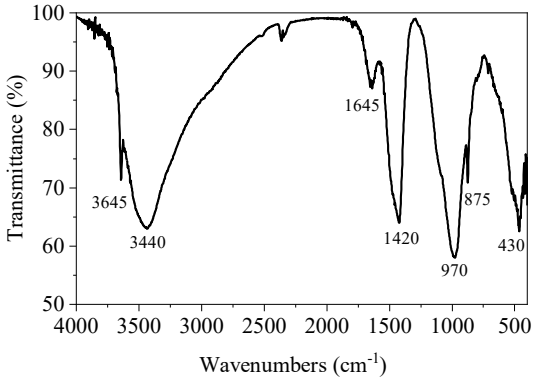

Fig. 9 FTIR spectra of the cement paste with 30% FBA-RMP as a replacement of cement after 28 days of curing

Pore structure

The cumulative/differential pore size distributions of the cement paste with 30% FBA-RMP as a replacement for cement after being cured for 28 days are shown on Fig. 10. The cement paste sample has a total porosity of approximately 19.72%, and the pores are concentrated in the range of 25 nm to 80 nm. In line with the widely accepted pore size classification for cement-based materials, pores are distinguished as fine pores (<50 nm), capillary pores (50–200 nm) and large pores (>200 nm). Accordingly, fine pores account for the dominant proportion, 71.7% of the total pores, while capillary pores constitute 9.03%. A considerable fraction of large pores is also observed, with a content as high as 19.27%. Such a distribution indicates that the pore structure is mainly composed of small-diameter pores, while the relatively high content of large pores reduces the compactness of the cement paste matrix.

Notably, trace metals (e.g., Al, Fe) residual in FBA-RMP may slightly react with water under the alkaline environment of cement hydration to generate H_2 (Saffarzadeh et al., 2011). However, most soluble impurities and free metal particles in FBA-RMP were removed through water immersion pretreatment in this study. Additionally, the ground FBA-RMP particles (≤75 μm) were tightly wrapped by hydration products during hydration, which significantly inhibited the reaction intensity between metals and water. Thus, the impact of H_2 gas production on the pore structure is limited, and the formation of large pores is mainly attributed to the inherent porous characteristics of FBA-RMP and the inhomogeneity of cement hydration rather than gas generation (Kleib et al., 2021).

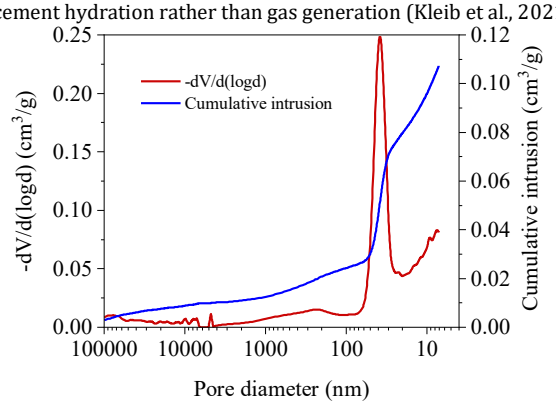

Fig. 10 The cumulative/differential pore size distributions of the cement paste with 30% FBA-RMP as a replacement of cement after 28 days of curing

Microscopic morphology

The microscopic morphology of the cement paste with 30% FBA-RMP as a replacement of cement after 28 days of curing is shown in Fig. 11. Unreacted FBA-RMP particles are observed in the cement paste, being tightly wrapped by hydration products, particularly the flocculent and amorphous C-S-H gel. This gel structure is the main contributor to the strength of the cement paste, and the finer particles from FBA-RMP can increase the compactness of the mixture and enhance its strength even if they do not react with cement. Additionally, distinct microcracks and obvious pores are visible in several locations in the sample, which may be attributed to the internal stress from hydration heat or volume shrinkage, and indicate that the FBA-RMP has a negative effect on the uniformity of cement hydration, which agrees with the findings of previous studies (Li et al., 2012).

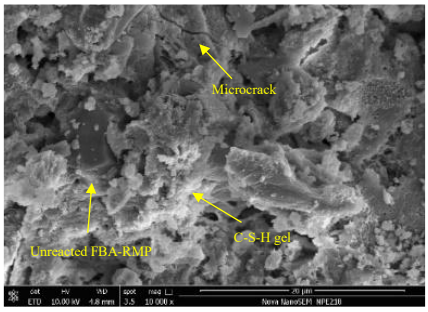

Fig. 11 The microscopic morphology of the cement paste with 30% FBA-RMP as a replacement of cement after 28 days of curing

3.3 Mortar properties

It has been reported that the reactivity of bottom ash from municipal solid waste incineration plants remains rather low. Consequently, its recycled micro-powder exhibits a delaying influence on the process of cement hydration. Li et al. (2012) confirmed that incorporating incineration bottom ash as a cement replacement would reduce the compressive strength of mortar, and the strength degradation became more significant with the increase of replacement level. To analyze the effects of FBA-RMP on the mechanical behavior of mortar, strength tests are carried out. The strengths of the mortar with 10%, 20%, 30% FBA-RMP instead of cement are shown in Fig. 12.

Replacing cement with 30% FBA-RMP significantly diminishes the compressive and flexural strengths of the mortar. The mortar cured for 28 days only possesses approximately 45.0% of the compressive strength of the reference specimens, far less than 70%. The flexural strength of the mortar performs significantly better than the compressive strength. The

application of 30% FBA-RMP as a cement substitute leads to a reduction of about 33.3% in the flexural strength of the mortar. This is due to the positive effect of the irregular particles in FBA-RMP on the flexural strength (Chen et al., 2011; Sheen et al., 2013), which acts as a filler in the mortar. The interlocking effect with the matrix provided by the inert FBA-RMP particles facilitates improving the flexural strength of the mortar. In conclusion, many hydration minerals such as C-S-H gel and AFt are identified in the cement paste containing 30% FBA-RMP after 28 days of curing. However, the participation of FBA-RMP in cement hydration is limited, and many pores are found in the cement paste, with large pores accounting for up to 19.27%. Therefore, although FBA-RMP contains oxides that are potentially reactive, they are primarily locked in crystalline phases with low pozzolanic activity. Consequently, FBA-RMP acts predominantly as an inert filler, which explains the significant reduction in mortar strength.

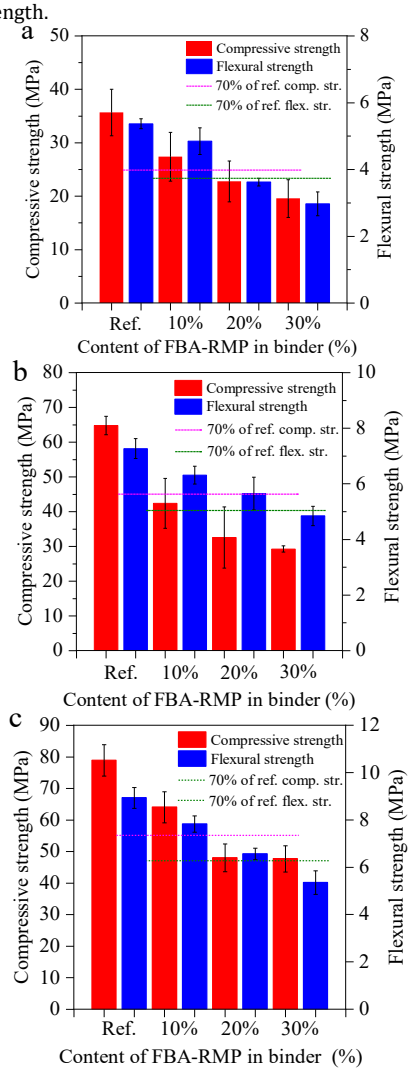

Fig. 12 Compressive and flexural strengths of the mortars after (a) 3, (b) 28 and (c) 90 days of curing

Decreasing the amount of FBA-RMP can reduce its negative effect on cement hydration. When it replaces 10% of the cement, the compressive and flexural strengths of the mortar cured for 28 days have respectively declined by 34.5% and 13.2% compared to those of the reference specimen. The influence of the curing days on the mechanical behavior of the mortar with FBA-RMP is relatively complex. For example, when FBA-RMP is used as a substitute for 30% of the cement, the 3-day compressive strength of the mortar is 19.6 MPa, which has declined by 45.2% compared to that of the reference specimen, and its performance is even better than that of the mortar cured for 28 days. This is related to the cement hydration process. At 3 days, less CH is released during cement hydration and fewer new minerals and gels are generated, resulting in an insignificant impact of FBA-RMP on the mortar strength. As time goes by, the cement hydration and reaction process speeds up, and the negative impact of FBA-RMP on the strength of the mortar increases, and the decline in the compressive strength of the mortar relative to the reference specimen becomes larger. However, with the increase in the curing days, more FBA-RMP participates in the reactions dominated by cement, and the compressive strength of the mortar is then improved. The 90-day compressive strength reaches 47.7 MPa, which has declined by 39.5% compared to that of the reference specimen. The influence of the curing days on the flexural strength of the mortar is obviously different from that on the compressive strength. The flexural strengths of the mortar with 30% FBA-RMP replacing cement at 3, 28 and 90 days have respectively declined by 44.7%, 33.3% and 40% compared to those of the reference specimen. This is because more FBA-RMP takes part in the hydration reaction while less serves as filler and interlocks with the matrix.

The pozzolanic activity of FBA-RMP was quantitatively characterized using the activity index (AI), a standard evaluation indicator for supplementary cementitious materials. According to the general definition for cementitious admixtures, the activity index at a given curing age is calculated as the percentage ratio of the compressive strength of FBA-RMP-containing mortar to that of the pure cement reference mortar. Based on the experimental results, the 28-day activity index of FBA-RMP at 30% replacement level is determined as 55.0%, while the 90-day activity index increases to 60.5%. The relatively low 28-day activity index indicates a limited early-age hydration degree of FBA-RMP. However, the noticeable increase in activity index with prolonged curing demonstrates that FBA-RMP contains effective active constituents, which can continuously participate in the hydration reaction with the calcium hydroxide released by cement hydration to generate additional C-S-H gel and AFt. This quantitative result is in good agreement with the identification of these hydration phases in the composite cement paste (Section 3.2.1), providing solid support for the statement that active constituents exist in FBA-RMP. A comparison with conventional supplementary cementitious materials (fly ash, ground granulated blast furnace slag, limestone powder) is not involved in this study, which is regarded as a limitation to be addressed in future work.

It should be noted that the experimental design of this study indirectly achieves the control of heavy metal-water reactions through multiple pathways, although no special tests were conducted for this purpose. Firstly, water immersion pretreatment removed some water-soluble heavy metal compounds along with impurities, reducing the reaction sites between heavy metals and water (Yao et al., 2010). Secondly, the FBA-RMP was ground to a particle size of ≤75 μm, and heavy metals were easily physically encapsulated by hydration products (e.g., C-S-H gel, AFt) during the hydration process, which reduced the contact probability between heavy metals and water. Thirdly, the replacement ratio of FBA-RMP was controlled within 30%, avoiding the intensification of reactions caused by the introduction of excessive heavy metals (Li et al., 2012). Existing studies have verified that similar pretreatment and application methods can effectively inhibit the leaching reaction of heavy metals in bottom ash (Yan et al., 2020), which provides indirect support for the environmental safety of this study.

3.4 Environmental impact evaluation

Hazardous substance leaching is crucial for the safe recycling of solid waste. A prior study evaluated the environmental impact of bottom ash ground micro-powder and its mortar (Cheng et al., 2024b), in which the leaching concentrations of heavy metals were investigated in accordance with GB 5085.3 (2007).

Inductively coupled plasma mass spectrometry (ICP-MS) was used to determine heavy metal concentrations in the leachates of the micro-powder and cement paste with 30% micro-powder replacing cement. Key results are summarized as follows. For the bottom ash ground micro-powder, the leaching concentrations of most heavy metals (As: 0.3943 mg/L, Cd: 0.0005 mg/L, Hg: 0.0003 mg/L, Ni: 3.7926 mg/L, Pb: 1.9682 mg/L, Zn: 9.1731 mg/L) met the standard limits, except for Cr (8.7173 mg/L, slightly exceeding the limit of 5 mg/L). However, after incorporating the micro-powder into cement paste (30% replacement ratio), the leaching concentrations of all heavy metals were significantly reduced (Cr: 2.3825 mg/L, Ni: 0.9574 mg/L, Pb: 0.6619 mg/L, Zn: 3.0479 mg/L, with others remaining at low levels), fully complying with the requirements of GB 5085.3 (2007).

This improvement in environmental safety is attributed to consistent pretreatment: the bottom ash was subjected to water immersion pretreatment to remove soluble impurities, and ground into a fine powder (≤75 μm) that can be tightly encapsulated by cement hydration products (e.g., C-S-H gel, AFt). These measures effectively inhibited the leaching of heavy metals, ensuring that the mortar containing bottom ash ground micro-powder posed no significant environmental risk during practical application.

4. Conclusion

1. Fine bottom ash recycled micro-powder (FBA-RMP) is classified in the SiO_2–CaO–Al_2O_3–Fe_2O_3 system, with these four oxides accounting for 85.3 wt.%. FBA-RMP contains low levels of Cl and SO_3, and its dominant crystalline phases are quartz and calcite, accompanied by gypsum, hematite, and magnetite.
2. In the cement paste with 30% FBA-RMP replacement cured for 28 days, C-S-H gel and AFt are formed, with the corresponding mass loss of gel-related water reaching 8.6%. Meanwhile, large pores account for 19.27% of the total pore structure.

3. The incorporation of FBA-RMP reduces the mechanical strength of mortar. A 30% replacement level causes a 55.0% decrease in 28-day compressive strength and a 33.3% reduction in flexural strength relative to the reference mortar, while 10% replacement lowers the 28-day compressive strength by 34.5%.
4. Prolonged curing improves the mortar strength: the 90-day compressive strength of mortar with 30% FBA-RMP is only 39.5% lower than that of the reference specimen, with the activity index increasing from 55.0% to 60.5%, suggesting an enhanced reactivity of FBA-RMP with extended curing time.

References

Abd Kadir, S.A.S., Yin, C.Y., Sulaiman, M.R., Chen, X. and El-Harbawi, M. (2013), "Incineration of municipal solid waste in Malaysia: salient issues, policies and waste-to-energy initiatives", Renewable and Sustainable Energy Reviews, 24, 181-186, https://doi.org/10.1016/j.rser.2013.03.041.

Bhardwaj, A., Kumar, S. and Singh, D. (2023), "Tannery effluent treatment and its environmental impact: a review of current practices and emerging technologies", Water Quality Research Journal, 58(2), 128–152, https://doi.org/10.2166/wqrj.2023.002.

Bosmans, A., Vanderreydt, I., Geysen, D. and Helsen, L. (2013), "The crucial role of waste-to-energy technologies in enhanced landfill mining: a technology review", Journal of Cleaner Production, 55, 10-23, https://doi.org/10.1016/j.jclepro.2012.05.032.

Cheng, L., Liu, W., Jin, H.S., Wu, Y.K., Ren, Y.R., Liu, J. and Xing, F. (2024a), "Influence of municipal solid waste incineration bottom ash particle size on the evolution mechanism and distribution characteristics of multiscale pore structures in cement paste", Construction and Building Materials, 452, 138882, https://doi.org/10.1016/j.conbuildmat.2024.138882.

Chen, M.Z., Lin, J.T., Wu, S.P. and Liu, C.H. (2011), "Utilization of recycled brick powder as alternative filler in asphalt mixture", Construction and Building Materials, 25(4), 1532-1536, https://doi.org/10.1016/j.conbuildmat.2010.08.005.

Cheng, Y.Z., Gao, G.H., Chen, L.J., Du, W.J., Mu, W.Y., Yan, Y.L. and Sun, H.S. (2024b), "Physical and mechanical study of municipal solid waste incineration (MSWI) bottom ash with different particle size distribution", Construction and Building Materials, 416, 135137, https://doi.org/10.1016/j.conbuildmat.2024.135137.

Fialova, J., Hybska, H., Samesova, D., Lobotkova, M. and Veverkova, D. (2019), "Assessment of the impact of municipal solid waste incineration bottom ash used as partial cement replacement in cement mixture using bioassays", Archives of Environmental Protection, 45(4), 104-113.

GB 5085.3. (2007), "Identification standards for hazardous wastes—Identification for extraction toxicity".

GB/T 17671. (2021), "Test Method of cement mortar strength".

Jin, H.S., Cheng, L., Liu, J., Chen, C.Y. and Xing, F. (2024), "Converting municipal solid waste incineration bottom ash into the value-added artificial lightweight aggregates through cold-bonded granulation technology", Construction and Building Materials, 438, 136930, https://doi.org/10.1016/j.conbuildmat.2024.136930.

Kleib, J., Aouad, G., Abriak, N.E. and Benzerzour, M. (2021), "Production of Portland cement clinker from French Municipal Solid Waste Incineration Bottom Ash", Case Studies in Construction Materials, 15, e00629, https://doi.org/10.1016/j.cscm.2021.e00629.

Kumar, S. and Singh, D. (2021), "Municipal solid waste incineration bottom ash: a competent raw material with new possibilities", Innovations in Infrastructure Solutions, 6, 201, https://doi.org/10.1007/s41062-021-00567-0.

Kumar, S. and Singh, D. (2023), "Transforming waste into sustainable solution: Physicochemical and geotechnical evaluation of cement stabilized municipal solid waste incinerator bottom ash for geoenvironmental applications", Process Safety and Environmental Protection, 176, 685–695, https://doi.org/10.1016/j.psep.2023.06.026.

Kumar, S. and Singh, D. (2024), "From waste to resource: Evaluating the possibility of incinerator bottom ash composites for geotechnical applications", International Journal of Environmental Science and Technology, 21(1), 703–714, https://doi.org/10.1007/s13762-023-04919-4.

Li, B.L., Wang, Y.H., Peng, D., Yang, L. and Zhang, Y.M. (2019), "Composition and Suitable Application of Electric Furnace Ferronickel Slag Sand and Ferronickel Slag Powder", Materials Reports, 33(22), 3752-3756.

Li, X.G., Lv, Y., Ma, B.G., Chen, Q.B., Yin, X.B. and Jian, S.W. (2012), "Utilization of municipal solid waste incineration bottom ash in blended cement", Journal of Cleaner Production, 32, 96-100, https://doi.org/10.1016/j.jclepro.2012.03.038.

Lin, K.L. and Lin, D.F. (2006), "Hydration characteristics of municipal solid waste incinerator bottom ash slag as a pozzolanic material for use in cement", Cement and Concrete Composites, 28(9), 817-823, https://doi.org/10.1016/j.cemconcomp.2006.03.003.

Liu, J., Ren, Y.R., Cheng, L., Jin, H.S. and Xing, F. (2025), "Unlocking the potential of municipal solid waste incineration bottom ash into sustainable fine aggregates for production of eco-friendly lightweight sprayed mortar", Journal of Building Engineering, 108, 112880, https://doi.org/10.1016/j.jobe.2025.112880.

Liu, J., Wu, Y.K., Cheng, L., Jin, H.S., Liu, J.Y. and Xing, F. (2024a), "Recycling of municipal solid waste incineration bottom ash (MSWIBA) particles into natural fine sands for sustainable engineering cementitious composites", Construction and Building Materials, 418, 135500, https://doi.org/10.1016/j.conbuildmat.2024.135500.

Liu, J., Wu, Y.K., Cheng, L., Jin, H.S., Li, J.X. and Xing, F. (2024b) "Assessment of mechanical and heavy metal leaching behavior of resource-efficient engineered cementitious composites incorporating ultra-high-volume municipal waste incineration bottom ash", Journal of Materials Research and Technology, 33, 5784–5808, https://doi.org/10.1016/j.jmrt.2024.10.205.

NBS (2023), "China Statistical Yearbook", China Statistics Press, Beijing, China.

Qiao, X.C., Tyrer, M., Poon, C.S. and Cheeseman, C.R. (2008), "Novel cementitious materials produced from incinerator bottom ash", Resources, Conservation and Recycling, 52(3), 496-510, https://doi.org/10.1016/j.resconrec.2007.06.003.

Ranjan, S., Singh, D. and Kumar, S. (2021), "Analysis of landfill leachate and contaminated groundwater: a review", in Proceedings of the Indian Geotechnical and Geoenvironmental Engineering Conference, Singapore: Springer Nature Singapore, pp. 55–62, https://doi.org/10.1007/978-981-19-4731-5_5.

Rehman, A.U., Lee, S.M. and Kim, J.H. (2020), "Use of municipal solid waste incineration ash in 3D printable concrete", Process Safety and Environmental Protection, 142, 219-228, https://doi.org/10.1016/j.psep.2020.06.018.

Saffarzadeh, A., Shimaoka, T., Wei, Y.M., Gardner, K.H. and Musselman, C.N. (2011), "Impacts of natural weathering on the transformation/neoformation processes in landfilled MSWI bottom ash: a geoenvironmental perspective", Waste Management, 31(12), 2440-2454, https://doi.org/10.1016/j.wasman.2011.07.017.

Sanjeev, K. and Deswal, S. (2021) "Comparative assessment of Kurukshetra city waste dumping sites using RIAM analysis: a case study", in Advances in Geo-Science and Geo-Structures: Select Proceedings of GSGS 2020, Singapore: Springer Singapore, pp. 31–38, https://doi.org/10.1007/978-981-16-1993-9_4.

Sheen, Y.N., Wang, H.Y., Juang, Y.P. and Le, D.H. (2013), "Assessment on the engineering properties of ready-mixed concrete using recycled aggregates", Construction and Building Materials, 45, 298-305, https://doi.org/10.1016/j.conbuildmat.2013.03.072.

Singh, D. and Kumar, S. (2022), "Physio-chemical Investigations on MSWI Bottom Ash for Sustainable Use", in Proceedings of the International Conference on Environmental Geotechnology, Recycled Waste Materials and Sustainable Engineering, Singapore: Springer Nature Singapore, pp. 87–95, https://doi.org/10.1007/978-981-99-4041-7_9.

Singh, D. and Kumar, S. (2023), "Challenges of municipal solid waste management in Jalandhar, Punjab (India): a case study", in Proceedings of the International Conference on Civil Engineering, Singapore: Springer Nature Singapore, https://doi.org/10.1007/978-981-99-4045-5_18.

Sisani, F., Maalouf, A. and Di Maria, F. (2022), "Environmental and energy performances of the Italian municipal solid waste incineration system in a life cycle perspective", Waste Management and Research, 40(2), 218-226.

Xu, Y.F., Fu, Y., Xia, W., Zhang, D., An, D. and Qian, G.R. (2018), "Municipal solid waste incineration (MSWI) fly ash washing pretreatment by biochemical effluent of landfill leachate: a potential substitute for water", Environmental Technology, 39(15), 1949-1954, https://doi.org/10.1080/09593330.2017.1345985.

Yan, K.Z., Sun, H. and You, L.Y. (2020), "Assessment and mechanism analysis of municipal solid waste incineration bottom ash as aggregate in cement stabilized macadam", Journal of Cleaner Production, 244, 118750, https://doi.org/10.1016/j.jclepro.2019.118750.

Yao, J., Li, W.B., Tang, M., Fang, C.R., Feng, H.J. and Shen, D.S. (2010), "Effect of weathering treatment on the fractionation and leaching behavior of copper in municipal solid waste incinerator bottom ash", Chemosphere, 81(5), 571-576, https://doi.org/10.1016/j.chemosphere.2010.08.038.

Disclaimer